Fatigue Testing/Materialography

S. Osman Yilmaz, Tanju Teker* and S. Süreyya Karabeyoğlu

Microstructure and fatigue performance of Cu-based M_7C_3-reinforced composites

https://doi.org/10.1515/mt-2021-2022

Abstract: Cu\Fe–Cr–C metal matrix composites (MMCs) were produced with a reinforcer addition of 6, 9, 12, 15, and 18 wt% Fe–Cr–C by powder metallurgy. The effects of sintering temperatures on Cu-based Fe–Cr–C-reinforced composites were studied using scanning electron microscopy (SEM), energy-dispersive spectroscopy (EDS), X-ray diffraction (XRD), and hardness test. The electrical conductivity and tensile and fatigue strengths of samples were investigated by the conductivity meter and the tensile and fatigue testing machine. The interface microstructure between Fe–Cr–C and Cu particulates at 1000 °C showed a significant difference. The increase in tensile strength, hardness, and fatigue life gave a proportional change with an increase in Fe–Cr–C particulate vol%. The precipitated carbides and intermetallic compositions reduced electrical resistivity depending on the sintering temperature.

Keywords: copper; fatigue testing; Fe–Cr–C; hardness; powder metallurgy.

1 Introduction

Copper–chromium (Cu–Cr) alloys with high electrical and mechanical strengths are used in materials such as electrical contacts and cables [1–3]. The Cu–Cr structure is a compound produced by the separation of a supersaturated Cu–Cr solid melt [4, 5]. Due to the solubility of Cr in Cu, rough unresolved Cr particles will cause performance degradation when there are Cr precipitates in the Cu matrix [6, 7]. There are many problems that can occur when preparing Cu–Cr alloys in a melting system. Since the dissolution movement of Cr into a Cu melt is quite late, it is necessary to increase the temperature to 1400 °C or a longer dissolution period. The problem between Cr and Cu is the large density difference (Cr = 7.19 g cm^{-3} and Cu = 8.95 g cm^{-3}). Therefore, solid Cr lightly floats on the surface of the Cu liquid. This indicates that Cr is hard to mix into the solution [7–9].

In addition, the floating Cr is easily repelled from the solution surface during the heating process. It becomes hotter due to stronger crossover with the induction field. So, it can act more easily with the pot wall. Therefore, there are distinct difficulties for this synthesis method, such as processing, quality, and high cost. Until now, much research on Cu–Cr alloys has aimed at improving their properties by adding diverse elements or thermomechanical treatments [10–13]. Fang et al. [14] reported that the properties of the Cu–Cr alloy are produced by mechanical grinding and alloying. The strong Cu/Cr interface and dissolved Cr atoms supported the reinforcement of the composite.

The aim of this study is to examine microstructure, hardness, tensile strength, fatigue life, and electrical conductivity for high-temperature studies of a new Cu–Fe–Cr–C alloy composite.

2 Experimental methods

The reinforcer was prepared as an Fe–Cr–C mixture of 64 wt% Cr, 24 wt% Fe, and 6 wt% C, and the size of the particulates were arranged approximately about 48 μm. The Cu powders (99.9% purity, 48 μm size) were selected as the test material. The composite and process conditions selected for the test samples are given in Table 1. The powders were mixed and homogenized in an alumina laboratory ball mill for 2 h at 120 rpm, and then cold-pressed uniaxially with a pressure of up to 200 MPa. Sintering temperatures were selected as 600–1000 °C temperature interval.

The samples were sanded using a series of SiC sandpapers from 180 to 2000 grit and polished with 1 μm diamond paste. For characterization of the microstructure, the samples were etched with a solution of 95 wt% $FeCl_3$ and 5 wt% HCl. The microstructural characterization of Cu-based Fe–Cr–C composite was determined using scanning electron microscopy (SEM: ZEISS EVO LS10) and energy-dispersive spectroscopy

***Corresponding author: Tanju Teker**, Sivas Cumhuriyet University, Faculty of Technology, Department of Manufacturing Engineering, 58140, Sivas, Turkey, E-mail: tanjuteker@cumhuriyet.edu.tr
S. Osman Yilmaz, Tekirdağ Namık Kemal University, Faculty of Engineering, Department of Mechanical Engineering, 59160, Çorlu, Tekirdağ, Turkey
S. Süreyya Karabeyoğlu, Kırklareli University, Faculty of Engineering, Department of Mechanical Engineering, 39020, Kırklareli, Turkey

Table 1: Processing conditions of the samples.

Sample no	S1	S2	S3	S4	S5	S6	S7	S8	S9	S10	S11	S12
Cu (wt%)	Bal.	Bal.	Bal.	Bal.	Bal.	Bal.	Bal.	Bal	Bal.	Bal.	Bal.	Bal.
Fe–Cr–C (wt%)	6	9	12	15	18	12	12	12	12	12	12	12
Sintering (°C)	900	900	900	900	900	600	700	800	850	900	950	1000

(EDS). Microhardness analysis was performed using a 50 g load at 0.5 mm intervals on the Vickers scale in the QNESS Q10 microhardness machine. Phase and carbide analyses with X-ray diffraction (XRD) were performed using a BRUKER brand device, 40 kV voltage, and 40 mA current. The electrical conductivity of the samples was investigated by a D60K-1201 conductivity meter. Tensile test samples were made according to the ASTM E8M–04 standards. The tensile test was performed using an Instron device. Fatigue experiments were performed on the INSTRON 8801 fatigue testing machine.

3 Results and discussion

3.1 Microstructural evaluation

The microstructure of Cu–Fe–Cr–C-alloyed S1, S2, S3, S4, and S5 samples consists primary M_7C_3 and $M_{23}C_6$ secondary carbides around Fe–Cr–C particles (Figure 1). In Figure 1a and b, primary $M_{23}C_6$ carbides precipitated as dark areas around Fe–Cr–C particles. M_7C_3 carbides occurred around the particles in lighter colors. Figure 1 shows primary α-dendrites with intermetallic compounds. Increasing the sintering temperature raised the melt ratio of the particles in the samples. Thus, the ratio of large primary M_7C_3 and secondary $M_{23}C_6$ precipitates increased. With the dispersion of C, Fe, and Cr particles into the matrix, several reactions and phases occurred in the diffusion zone. The microstructure images in Figure 1 show the distribution of Cr in the Cu matrix containing distinct Cu/Fe–Cr–C ratio. The microstructure of the S1 alloy was composed of a Cr-rich particle in a Cu dense matrix. According to the quantity of Cr in S1, the temperature distinction between liquid and solid was close, and Cr atoms could be maximally dissolved in Cu-rich solid solution. As the Cr quantity increased, larger phase regions nucleated. This led to the formation of more Cr-rich phases before the existence of Cu-rich supersaturated solid solution. Significant changes in the microstructure are seen in Figure 1b and c. The increase in Cr content caused major roughing of Cr-rich Cu particles. The dimension and density of the Cr-rich particles increased. Abnormal forms of Cr particles were obtained at S2. This was an indication that some Cr powders were not crystallized to carbide by nucleation and crystal growth. Cr-rich Cu particles are formed at around 330 °C and 630 °C and are combined with the Cu matrix. Diffusion increased as the temperature increased, and due to the less melting time and temperature, some Fe–Cr–C particles do not refuse into the Cu melt. Fe–Cr–C particles diffuse into the Cu matrix and eventually form these anomalies. The morphology of fine particles was found to be round in SEM micrographs. Ultrafine particles were formed by diffusion along the sintering operation. During sintering, it took a clear time to drop the sample temperature to 400 °C. In Cu–Cr alloys, the precipitation and growth of Cr particles begin at 400 °C. Due to high supersaturation of the Cu-rich phase in S2 and S3, the Cr particles precipitated and developed to form these ultrafine particles during this period.

The microstructures consist of precipitated $M_{23}C_6$-M_7C_3 carbides around Cr particles over 600 °C sintering temperature; in other words, precipitation of carbides started over 600 °C sintering temperature. The reinforcement particles can be divided into primary particles (40–50 μm) and secondary precipitated carbides (5–20 μm). With the increasing sintering temperature, M_7C_3-MC carbides were fully crystallized from Cr–Fe–C particles, and the microstructure presented minor secondary precipitated carbide. At higher sintering temperatures, greater amounts of secondary carbides were formed.

X-ray diffractions of S1 and S5 samples are given in Figure 2a and b. $M_{23}C_6$, M_7C_3 carbides, and α–Cu phase appeared in the samples. The M_7C_3 intensity in samples increased over 800 °C sintering temperature, and over 950 °C, the $M_{23}C_6$ carbides almost eliminated. The amount of $M_{23}C_6$ in S2 and S3 are higher than that in S4 and S5. The precipitated carbides in the samples were determined as minor rates of Cr_7C_3 and mostly M_7C_3. The chemical composition of M_7C_3 was detected as (M = Fe, Cr) by EDS (Figure 3). Also, residual stresses occurred at grain boundaries. The cause of residual stress formation in the grain nucleus was carbide precipitation. During the sintering process, the matrix grains were in the wider direction and were limited by the grain boundary nucleus [14, 15].

Element concentrations in the matrix of samples are presented in Figure 3 by EDS analysis. Cr, Fe, and C atoms

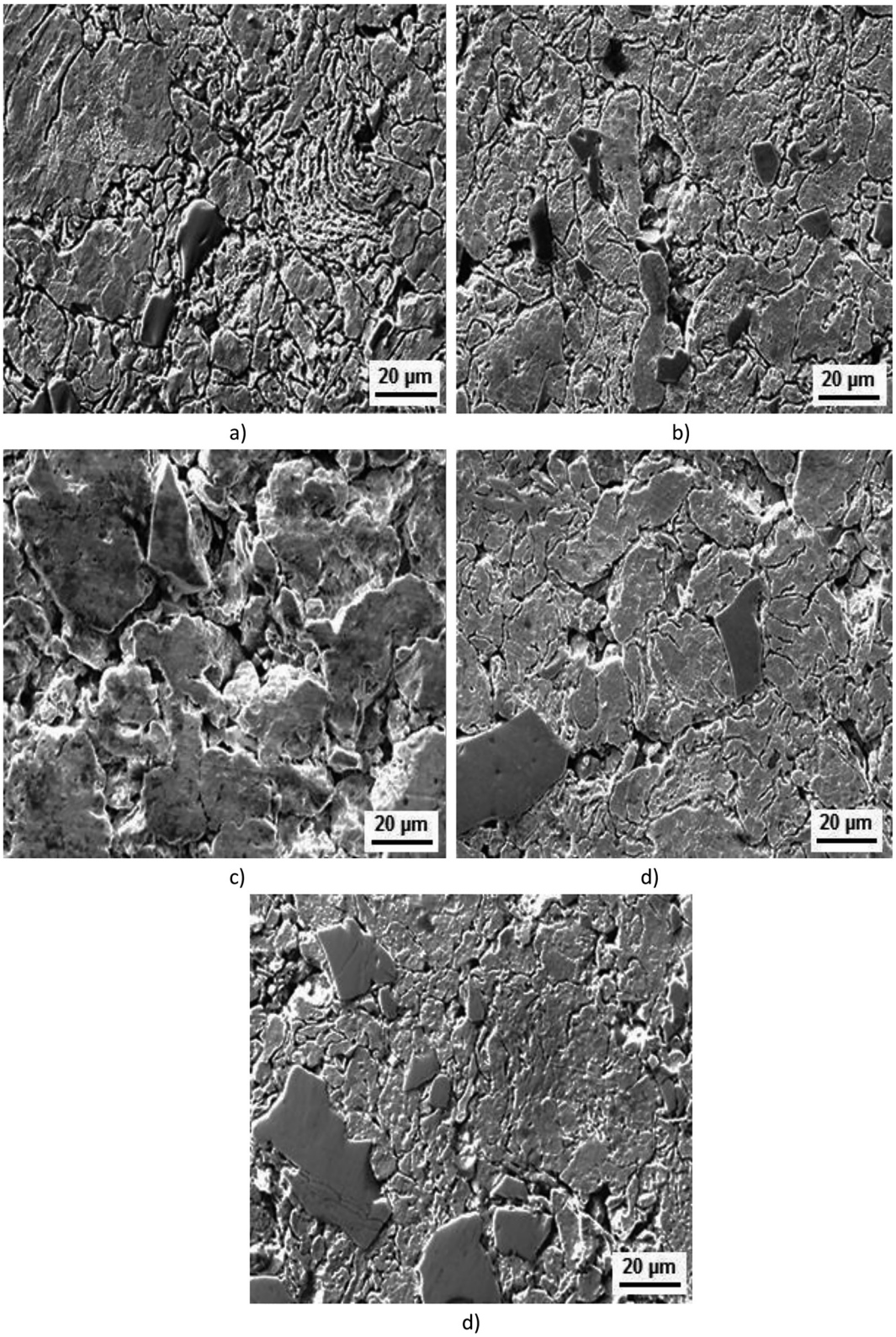

Figure 1: Scanning electron microscopy (SEM) micrographs of the experiment samples, a) S1, b) S2, c) S3, d) S4, e) S5.

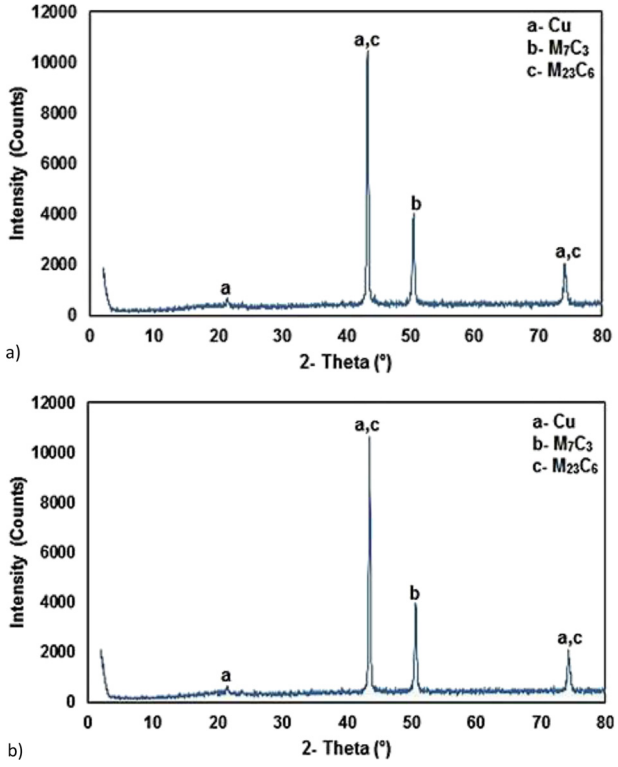

Figure 2: X-ray diffraction (XRD) pattern of samples, a) S1, b) S5.

were transferred into the grains by diffusion. Cr and Fe concentrations decreased toward the center of the Cu particles. An increase in the content of Fe–Cr–C raised the diffusion quantity of Cr and Fe and their concentration in Cu particles. The rise in the Fe–Cr–C quantity increased the Cu content in the carbides. The increase in Fe–Cr–C percentage due to the diffusion of Cu atoms in the Fe–Cr–C also increased the number of grain boundary carbides. This rise in the particle ratio lowered the dissolution heat of the particles [16, 17]. Thus, the activation energy of the Cr atoms increases. This raised the diffusion quantity of Cr atoms from Fe–Cr–C into the matrix. The decrease in Fe–Cr–C particle size in the microstructure was due to the increase in diffusion quantity of Cr and Fe. Therefore, as the particle ratio increased, the intensity of Cr and Fe particles in the matrix enhanced.

Microhardness of test samples is given in Figure 4 for a cross-sectional area for 900 μm distance from the surface. The hardness increased with increasing Fe–Cr–C percentage. The increase in hardness was due to the increase in the amount of $M_{23}C_6$-M_7C_3 carbide in the Cu matrix and the transfer of Cr, Fe, and C atoms to the matrix. The effect of Fe/Cr on surface hardness is shown in Table 2. As the particle ratio increased, the surface hardness and fatigue limit increased [18, 19]. The elongation was decreased as the Fe–Cr–C content increases. The increase in the Fe–Cr–C content together with the increase in the $M_{23}C_6$ carbide ratio formed at the grain boundary and the increase in the hardness of the matrix decreased the elongation (Table 2).

3.2 Fatigue and tensile strength

Mechanical test results of the materials are given in Table 2. The tensile strength and hardness increased, and the % elongation declined due to the dissolution of Fe–Cr–C, the diffusion of Fe–Cr–C particles in the matrix, and the primary M_7C_3 and secondary $M_{23}C_6$ carbides. The increase in hardness, tensile strength, and fatigue strength was proportional to the increase in Fe–Cr–C reinforcer volume content (Figure 5a and b). This rise in tensile and fatigue strength due to dissolution of Fe–Cr–C was affected by the reduction in the size of Fe–Cr–C particles [20–22].

The concentration of reinforcer increased the fatigue limit and hardness linearly; on the other hand, tensile strength increased parabolically. S-N curves of Cu/Fe–Cr–C alloys are given in Figure 6. Fatigue life of the samples was raised with the dissolution of Fe–Cr–C concentration. Increasing the ratio of Fe/Cr particles potently advanced the fatigue crack initiation point to the grain boundary. Thus, more stress had to be applied to the surface to produce a sufficiently high stress level at the grain boundary to cause fatigue cracking.

The fatigue fracture surfaces of S1 and S5 samples are given in Figure 7a and b. Fatigue cracks caused by Cu/Fe–Cr–C were in the form of “fish eyes” in all of the broken samples. The results showed that the carbides had no significant effect on the starting and spread of fatigue cracks. Increasing the Cu/Fe–Cr–C quantity increased the fatigue limit of MMC.

3.3 Electrical resistivity

The relation between Fe–Cr–C particulates and electrical resistance – sintering temperature are presented in Figure 8. The electrical conductivity of the samples was raised by the sintering temperature. The electrical conductivity of metals is related to the contacts of electrons with crystalline phonons, soluble atoms, and crystal structure defects at room

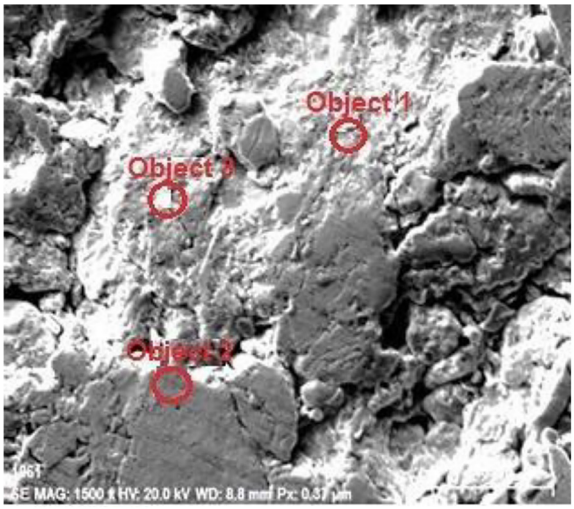

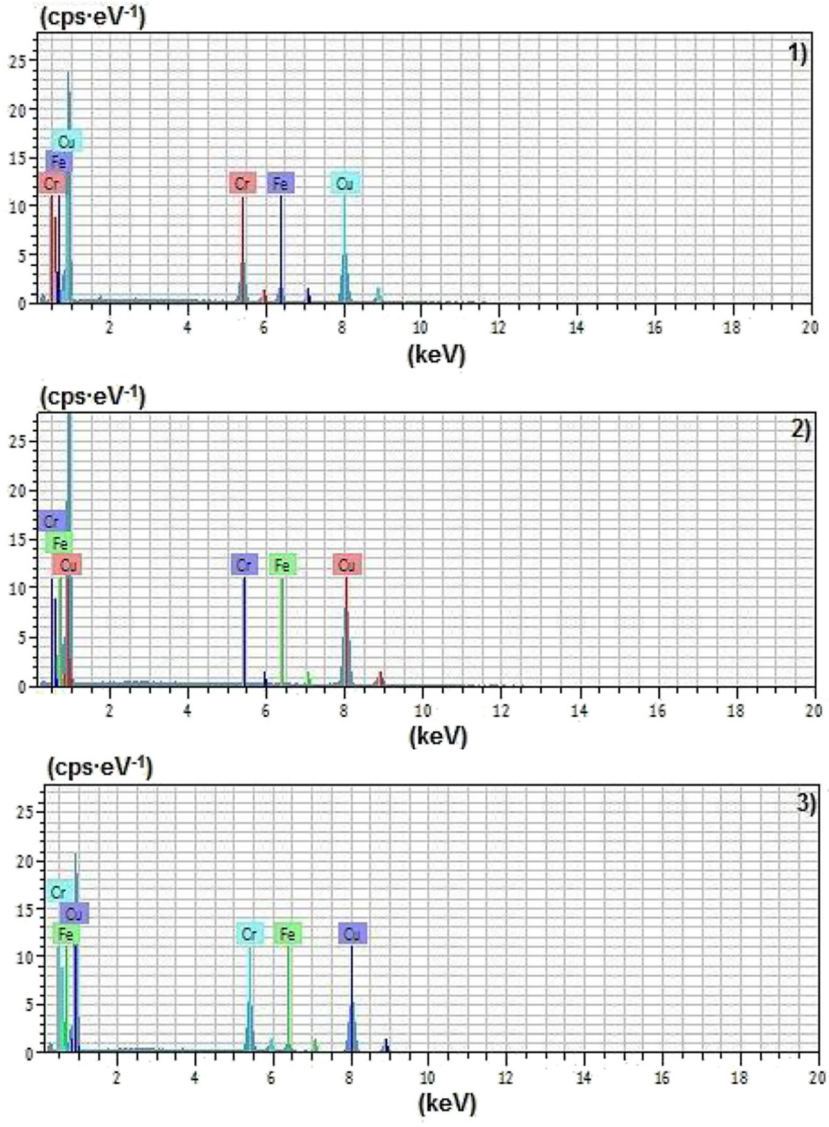

Figure 3: Energy-dispersive spectroscopy (EDS) analysis results of sample S5.

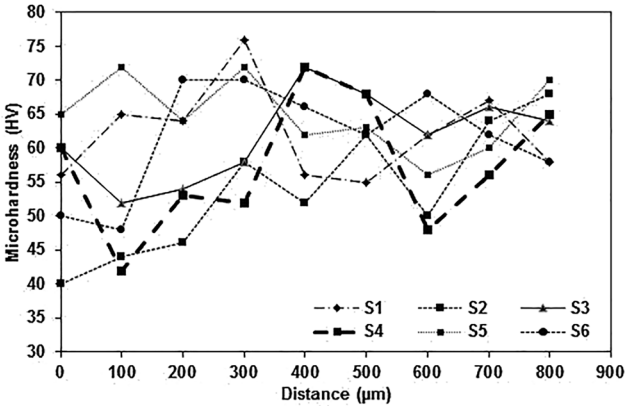

Figure 4: Microhardness of test samples.

Table 2: Mechanical test results of the materials.

Material	Tensile strength (MPa)	Yield strength (MPa)	Elongation (%)	Surface hardness HV	Fatigue strength (MPa)
S1	282	218	12	63	20
S2	298	226	10	112	32
S3	315	284	8	201	46
S4	340	293	5	263	63
S5	452	405	3	306	89

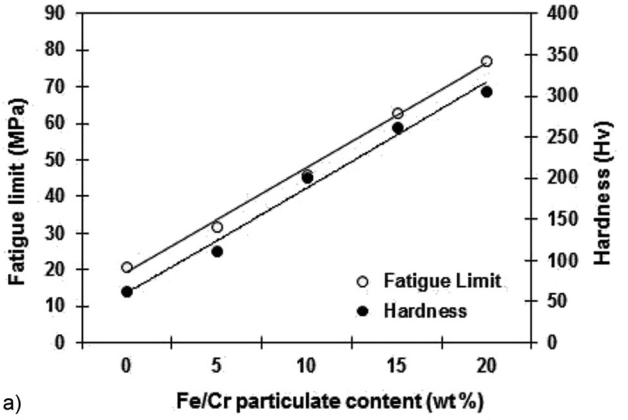

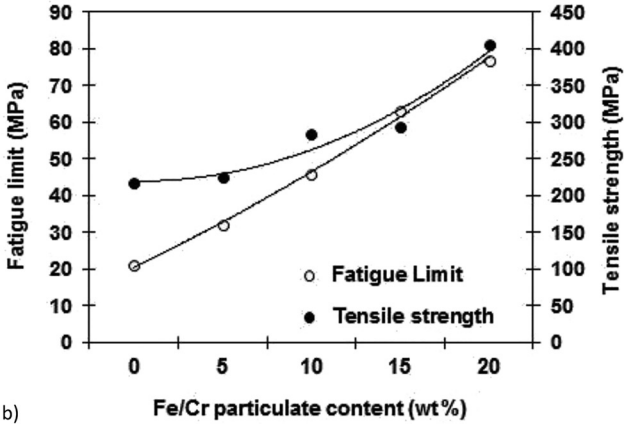

Figure 5: The relation in hardness, tensile strength, and fatigue strength of Fe–Cr–C content, a) hardness and fatigue strength, b) fatigue and tensile strength.

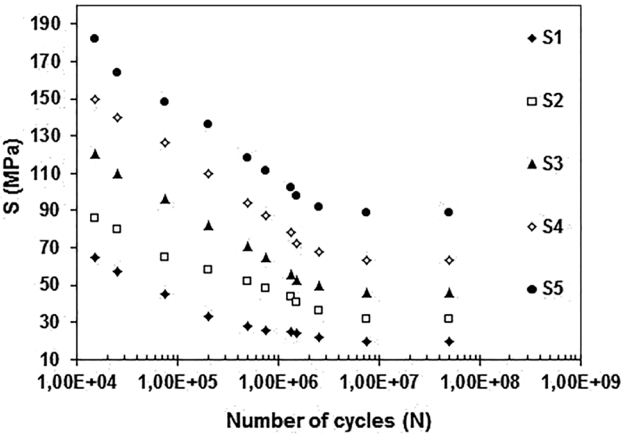

Figure 6: S-N curves for Cu–Fe–Cr–C alloys.

temperature [23]. The rise in electrical resistance of samples was related to the increase in the Fe–Cr–C concentration and sintering temperature. The rise in particulate quantity declined the dependence of electrical resistivity to temperature. Precipitated carbides and intermetallic compositions reduced electrical resistance. The rise in atomic vibration translates the energy received by electrons from outside into heat under the influence of an electric field. The thermal energy is then diffused into the sample as temperature. Thus, as the vibration in the crystal structure increases, the temperature of the sample rises, and the free road received by the electrons reduces. However, in the event of a collision, the waves will disperse, and the speed will decrease [23–26]. With the increase in the Fe–Cr–C ratio, the amount of collision increased, the wave scattered, and the net current flow rate reduced. The electrical resistivity was impressed by particle addition and sintering temperature in the polynomial function. The increase in sintering temperature decreased electrical resistivity due to the decrease of voids in the microstructure. The concentration of Cr-rich Cu particles increased during sintering at 750–1000 °C. As the temperature increased, diffusion increased, and Fe–Cr–C particles diffused into the Cu matrix and eventually formed the fine carbide particulates which affected the electrical resistivity also (Figure 8). The morphology of fine particles affected the electrical resistivity as a polynomial.

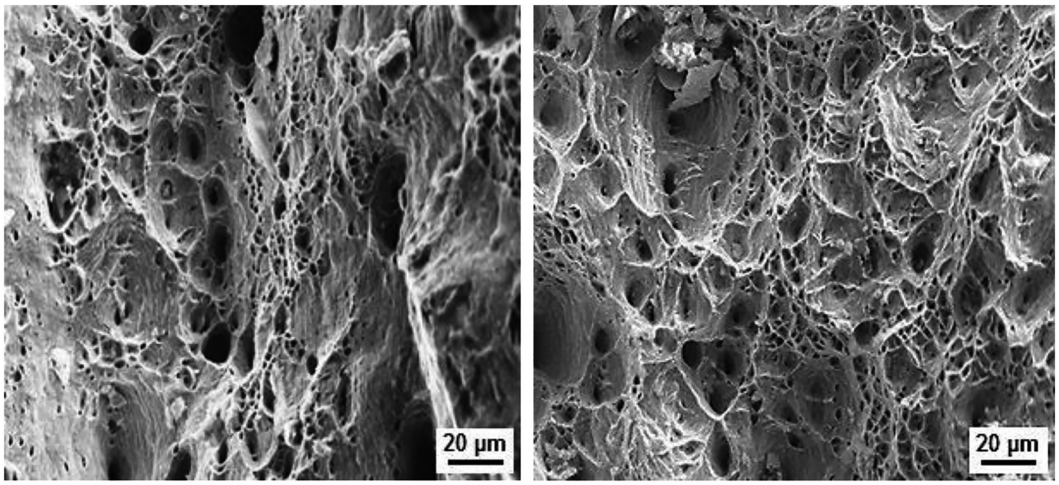

Figure 7: The fatigue fracture surface of samples, a) S1, b) S5.

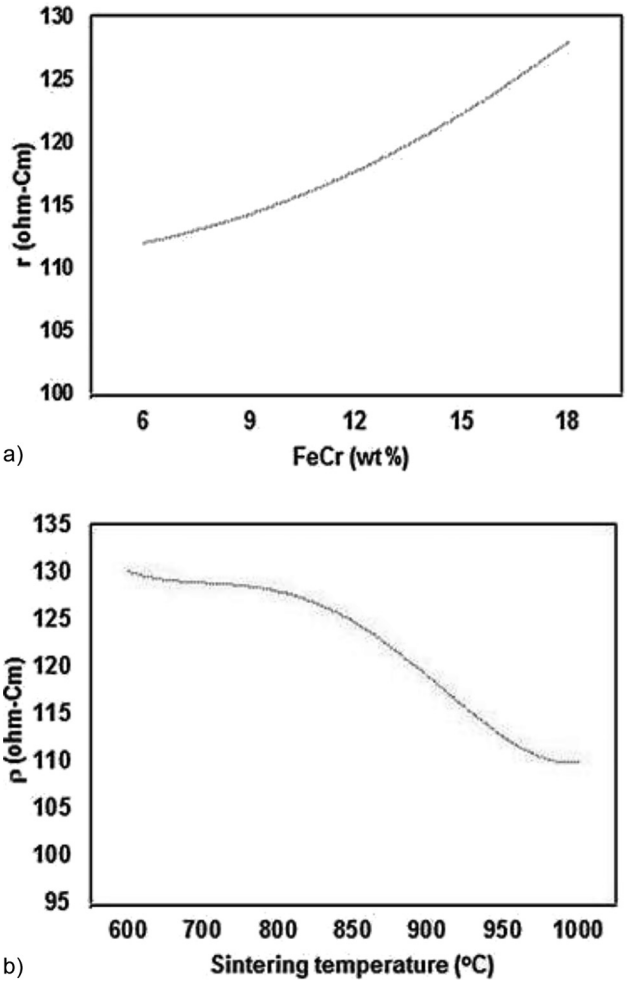

Figure 8: Dependence of electrical resistance from, a) Fe–Cr–C particles, b) sintering temperature.

4 Conclusions

The most important conclusions of the research are as follows:

- The increase in the Cu/Fe–Cr–C particle ratio changed the overall structure.
- The microstructure of Cu–Fe–Cr–C alloy samples occurred from primary M_7C_3 and $M_{23}C_6$ secondary carbides around Fe–Cr–C particles dispersed in Cu.
- The amount of precipitated $M_{23}C_6$ and M_7C_3 carbides increased depending on the Cu/Fe–Cr–C particulate percentage and sintering temperature. The increase in sintering temperature increased the $M_7C_3/M_{23}C_6$ ratio.
- The increase in tensile, hardness and fatigue capacity gave a proportional change with increase in the Fe/Cr particulate vol%.
- The fatigue capacity increased with the dissolution of Fe–Cr–C particles.
- The carbides and intermetallic phases declined electrical resistivity depending on the sintering temperature.
- The rise in the Cu/Fe–Cr–C amount reduced the dependence of electrical resistivity to temperature.

Acknowledgment: The authors are grateful to KAYALAR copper industry and trade incorporated company for their assistance in conducting the experiments.

Author contributions: All the authors have accepted responsibility for the entire content of this submitted manuscript and approved submission.

Research funding: None declared.

Conflict of interest statement: No potential conflict of interest was reported by the authors.

References

[1] N. F. Shkodich, A. S. Rogachev, S. G. Vadchenko, et al., "Bulk Cu-Cr nanocomposites by high-energy ball milling and spark plasma sintering," *J. Alloys Compd.*, vol. 617, pp. 39–46, 2014, https://doi.org/10.1016/j.jallcom.2014.07.133.

[2] Q. Fang and Z. X. Kang, "An investigation on morphology and structure of Cu-Cr alloy powders prepared by mechanical milling and alloying," *Powder Technol.*, vol. 270, pp. 104–111, 2015, https://doi.org/10.1016/j.powtec.2014.10.010.

[3] D. P. Shena, Y. J. Zhu, X. Yang, and W. P. Tong, "Investigation on the microstructure and properties of Cu-Cr alloy prepared by in-situ synthesis method," *Vacuum*, vol. 149, pp. 207–213, 2018, https://doi.org/10.1016/j.vacuum.2017.12.035.

[4] J. M. Zhou, D. G. Zhu, L. T. Tang, et al., "Microstructure and properties of powder metallurgy Cu-1%Cr-0.65%Zr alloy prepared by hot pressing," *Vacuum*, vol. 131, pp. 156–163, 2016, https://doi.org/10.1016/j.vacuum.2016.06.008.

[5] I. S. Batra, G. K. Dey, U. D. Kulkarni, and S. Banerjee, "Precipitation in a Cu–Cr–Zr alloy," *Mater. Sci. Eng.*, vol. 356, nos. 1–2, pp. 326–336, 2003, https://doi.org/10.1016/S0921-5093(02)00852-3.

[6] Y. Wang, B. H. Tang, and F. Y. Li, "The properties of self-formed diffusion barrier layer in Cu(Cr) alloy," *Vacuum*, vol. 126, pp. 51–54, 2016, https://doi.org/10.1016/j.vacuum.2016.01.019.

[7] C. Watanabe, R. Monzen, and K. Tazaki, "Mechanical properties of Cu-Cr system alloys with and without Zr and Ag," *J. Mater. Sci.*, vol. 43, pp. 813–819, 2008, https://doi.org/10.1007/s10853-007-2159-8.

[8] L. X. Sun, N. R. Tao, and K. Lu, "A high strength and high electrical conductivity bulk CuCrZr alloy with nanotwins," *Scripta Mater.*, vol. 99, pp. 73–76, 2015, https://doi.org/10.1016/j.scriptamat.2014.11.032.

[9] N. Gao, E. Huttunen-Saarivirta, T. Tiainen, and M. Hemmilä, "Influence of prior deformation on the age hardening of a phosphorus-containing Cu-0.61 wt% Cr alloy," *Mater. Sci. Eng.*, vol. 342, nos. 1–2, pp. 270–278, 2003, https://doi.org/10.1016/S0921-5093(02)00306-4.

[10] W. X. He, E. D. Wang, L. X. Hu, Y. Yu, and H. F. Sun, "Effect of extrusion on microstructure and properties of a submicron crystalline Cu–5 wt% Cr alloy," *J. Mater. Process. Technol.*, vol. 208, nos. 1–3, pp. 205–210, 2008, https://doi.org/10.1016/j.jmatprotec.2007.12.107.

[11] Z. M. Zhou, Y. P. Wang, J. Gao, and M. Kolbe, "Microstructure of rapidly solidified Cu 25 wt% Cr alloys," *Mater. Sci. Eng., A*, vol. 398, nos. 1–2, pp. 318–322, 2005, https://doi.org/10.1016/j.msea.2005.03.095.

[12] D. Seo, K. Ogawa, and K. Sakaguchi, "Parameter study influencing thermal conductivity of annealed pure copper coatings deposited by selective cold spray processes," *Surf. Coating. Technol.*, vol. 206, nos. 8–9, pp. 2316–2324, 2012, https://doi.org/10.1016/j.surfcoat.2011.10.010.

[13] K. X. Wei, W. Wei, F. Wang, Q. B. Du, I. V. Alexandrov, and J. Hua, "Microstructure, mechanical properties and electrical conductivity of industrial Cu–0.5%Cr alloy processed by severe plastic deformation," *Mater. Sci. Eng.*, vol. 528, no. 13, pp. 1478–1484, 2011, https://doi.org/10.1016/j.msea.2010.10.059.

[14] Q. Fang, Z. X. Kang, Y. W. Gan, and Y. Long, "Microstructures and mechanical properties of spark plasma sintered Cu-Cr composites prepared by mechanical milling and alloying," *Mater. Des.*, vol. 88, pp. 8–15, 2015, https://doi.org/10.1016/j.matdes.2015.08.127.

[15] X. Sauvage, P. Jessner, F. Vurpillot, and R. Pippan, "Nanostructure and properties of a Cu–Cr composite processed by severe plastic deformation," *Scripta Mater.*, vol. 58, no. 12, pp. 1125–1128, 2008, https://doi.org/10.1016/j.scriptamat.2008.02.010.

[16] C. Masuda and Y. Tanaka, "Fatigue properties of Cu–Cr in situ composite," *Int. J. Fatig.*, vol. 28, no. 10, pp. 1426–1434, 2006, https://doi.org/10.1016/j.ijfatigue.2006.02.051.

[17] J. C. Pang, S. X. Li, Z. G. Wang, and Z. F. Zhang, "General relation between tensile strength and fatigue strength of metallic materials," *Mater. Sci. Eng.*, vol. 564, pp. 331–341, 2013, https://doi.org/10.1016/j.msea.2012.11.103.

[18] L. Cai, X. Jiang, Y. Guo, et al., "Friction and wear performance of a copper-based bond emery wheel for rail grinding," *Mater. Test.*, vol. 62, no. 12, pp. 1205–1214, 2020, https://doi.org/10.3139/120.111594.

[19] D. Uzunsoy, E. Kelesoglu, and Y. Erarslan, "Contribution of MoS2 additives to the microstructure and properties of pm copper based brake material," *Mater. Test.*, vol. 51, no. 5, pp. 318–322, 2009, https://doi.org/10.3139/120.110040.

[20] W. Wang, W. Yan, Q. Duan, Y. Shan, Z. Zhang, and K. Yang, "Study on fatigue property of a new 2.8 GPa grade steel," *Mater. Sci. Eng.*, vol. 527, nos. 13–14, pp. 3057–3063, 2010, https://doi.org/10.1016/j.msea.2010.02.002.

[21] A. Vinogradov and S. Hashimoto, "Multiscale phenomena in fatigue of ultra-fine grain materials- an overview," *Mater. Trans.*, vol. 42, no. 1, pp. 74–84, 2001, https://doi.org/10.2320/matertrans.42.74.

[22] G. Khatibi, J. Horky, B. Weiss, and M. J. Zehetbauer, "High cycle fatigue behaviour of copper deformed by high pressure torsion," *Int. J. Fatig.*, vol. 32, no. 2, pp. 269–278, 2010, https://doi.org/10.1016/j.ijfatigue.2009.06.017.

[23] J. C. Pang, Q. Q. Duan, S. D. Wu, S. X. Li, and Z. F. Zhang, "Fatigue strengths of Cu–Be alloy with high tensile strengths," *Scripta Mater.*, vol. 63, no. 11, pp. 1085–1088, 2010, https://doi.org/10.1016/j.scriptamat.2010.08.009.

[24] A. R. Boccaccini, "Predicting the electrical conductivity of two-phase composite materials," *Scripta Mater.*, vol. 36, no. 10, pp. 1195–1200, 1997, https://doi.org/10.1016/S1359-6462(97)00017-1.

[25] S. F. Abbas, S. J. Seo, K. T. Park, B. S. Kim, and T. S. Kim, "Effect of grain size on the electrical conductivity of copper–iron alloys," *J. Alloys Compd.*, vol. 720, pp. 8–16, 2017, https://doi.org/10.1016/j.jallcom.2017.05.244.

[26] G. A. Jerman, I. E. Anderson, and J. D. Verhoven, "Strength and electrical conductivity of deformation–processed Cu–15 vol Pct Fe alloys produced by powder metallurgy techniques," *Metall. Trans. A*, vol. 24, no. 1, pp. 35–42, 1993, https://doi.org/10.1007/BF02669600.

The authors of this contribution

S. Osman Yilmaz
Prof. Dr. S. Osman Yilmaz, born in Elazig in 1966, works at the University of Namık Kemal, Faculty of Engineering, Department of Mechanical Engineering, Corlu, Tekirdağ, Turkey. He received his B.Sc. from METU University, Ankara, Faculty of Engineering, Metallurgy and Materials Engineering Department in 1989; his M.Sc. from the Institute of Science and Technology, Metallurgy Department in 1992; and his Ph.D. from the University of Firat, Institute of Science and Technology, Metallurgy Department, Elazig in 1998. He studied metal coating techniques, surface modification, welding, casting, and wear.

Tanju Teker
Prof. Dr. Tanju Teker, born in Sivas in 1971, works in University of Sivas Cumhuriyet, Faculty of Technology, Department of Manufacturing Engineering, Sivas, Turkey. He graduated in Metallurgy Education from Gazi University, Ankara, Turkey, in 1997. He received his M.Sc. and Ph.D. degrees from Firat University, Elazig, Turkey, in 2004 and 2010, respectively. His research interests metal coating techniques, casting, fusion, and welding solid-state welding methods.

S. Süreyya Karabeyoğlu
Assist. Prof. Dr. S. Süreyya Karabeyoğlu, born in 1982, works at the University of Kırklareli, Faculty of Engineering, Department of Mechanical Engineering, Kırklareli, Turkey. He graduated in Mechanical Engineering from Dumlupınar University, Kütahya, Turkey, in 2004. He received his M.Sc. and Ph.D. degrees from Trakya University, Edirne, Turkey, and Namık Kemal University, Tekirdağ, Turkey, in 2007 and 2012, respectively. His research interests material design and behaviors, composite materials, and production technologies.